

# Superfluid He in Rotation: Single-Vortex Resolution and Requirements on Rotation

R. Blaauwgeers,<sup>1,2</sup> S. Boldarev,<sup>1,3</sup> V. B. Eltsov,<sup>1,3</sup> A. P. Finne,<sup>1</sup> and M. Krusius<sup>1</sup>

<sup>1</sup> Low Temperature Laboratory, Helsinki University of Technology, P.O. Box 2200, FIN-02015 HUT, Finland

E-mail: krusius@neuro.hut.fi

<sup>2</sup> Kamerlingh Onnes Laboratory, Leiden University, P.O. Box 9504, 2300 RA Leiden, The Netherlands

<sup>3</sup> Kapitza Institute for Physical Problems, 119334 Moscow, Russia

(Received November 1, 2002; revised April 22, 2003)

*The present generation of rotating refrigerators, which are used for the study of quantized vorticity in helium superfluids, are often capable of cooling to mK temperatures and rotate up to  $\sim 1$  rev/s. To achieve single-vortex resolution at all rotation velocities, smooth and stable rotation is required. This calls for low and stable rotational friction, sufficient axial alignment and lateral balancing of weights, to promote mechanical stability and precession-free rotation. We comment on general design principles, discuss the rotation noise spectrum of our installation, and describe interference problems from the rotation in low-noise measurement.*

**KEY WORDS:** air bearings; single-vortex resolution; rotation.

## 1. ROTATION IN <sup>3</sup>He RESEARCH

Starting from the nineteen forties, rotation has been one tool to investigate superfluid flow and quantized vortex lines in <sup>4</sup>He-II.<sup>1-3</sup> Later also other methods were introduced, such as thermally excited counterflow of the normal and superfluid fractions or the generation of flow via the motion of solid objects. These later techniques have often turned out to be technically simpler to implement and sometimes more effective.

However, there exist specialized areas where rotation has become an indispensable tool. One of these is the study of vortex structures in <sup>3</sup>He

superfluids. A number of reasons have contributed to this development: (i) Many different structures of vorticity exist which can be generated and studied in rotation.<sup>4</sup> (ii) Owing to the large superfluid coherence length  $\xi(T, p) > 10$  nm, vortex pinning on solid surfaces and remanent vorticity do not play as important a role as in <sup>4</sup>He-II. Thus vortex formation and annihilation processes can be investigated in detail.<sup>5,6</sup> (iii) The critical velocities are relatively high, they are governed to a large extent by intrinsic phenomena and to a lesser degree by the surface properties of the container wall. This allows also the study of rotating vortex-free states and their unusual properties.<sup>7</sup> Thus rotating superfluid <sup>3</sup>He measurements have uncovered a large number of new phenomena, which have provided the first detailed illustrations of quantized vorticity in anisotropic fermion superfluids. It is inconceivable to imagine that superconductors could be investigated only at zero external field: It has become evident that rotation is as important in the study of the <sup>3</sup>He superfluids, their multi-component order-parameter fields, and the multitude of topologically stable defects which can exist there.

Thirty years have passed since the discovery of the <sup>3</sup>He superfluids and twenty since the first measurements on their quantized vortices in uniform rotation. Nevertheless, many questions remain unanswered. Virtually nothing is known about vortex structures in restricted geometries.<sup>8</sup> Such measurements require high rotation velocities and sensitive measuring techniques. One to three orders of magnitude higher rotation velocities than those of today would be important to explore also from another point of view: The influence of high-velocity rotation on Cooper pairing has been predicted to lead to phase transitions and changes in vortex structure.<sup>9</sup> A further unexplored area is turbulence, where especially interesting today is the nature of the dissipation mechanisms in the zero temperature limit.<sup>10</sup> Significant questions of this magnitude have not been studied systematically, partially because of a lack of efficient methods. A good example is superfluid turbulence, where rotating measurements do not seem to have contributed lately: Rotation clearly provides possibilities for calibrating measuring signals in the presence of a known vortex structure, number of vortex lines and their overall configuration, but it is less obvious whether rotation can be efficiently used to generate turbulence.

In addition to higher velocities, our own experience has underlined the need for rotation of sufficiently good quality. Stable rotation is required in measurements of critical velocities with single-vortex resolution or to determine the number of circulation quanta per vortex line. By good fortune, our rotating refrigerator (called Helsinki I in Table I) has proven adequate for such purposes. Lately, however, the question of improvements has arisen: Can the maximum safe rotation velocity be increased or the

rotation noise be reduced? To provide answers, measurements of the rotation properties were performed. This report describes the results, but leaves the solutions for improvements so far open. After a brief digression into the general design solutions of various existing rotating cryostats we proceed to discuss the rotation characteristics of the Helsinki I machine.

## 2. ROTATING REFRIGERATOR DESIGN

Rotating mK refrigerators have evolved from standard laboratory cryostats with a  $^3\text{He}$ - $^4\text{He}$  dilution machine as pre-cooler and a nuclear demagnetization stage for cooling the sample. To operate a dilution refrigerator in rotation requires new design solutions. Rotation also introduces difficulties of more general nature: (i) increased heat leaks from unstable noisy rotation or from magnetic fields which are stationary in the laboratory, such as the lateral component of the earth's field, and (ii) interference and noise in sensitive measurements. With presently proven techniques smooth rotation, within  $\pm 1 \cdot 10^{-3}$  rad/s from the mean, is achievable up to rotation velocities of order  $\Omega \sim 10$  rad/s. Simultaneously the total heat leak to the nuclear cooling stage can be maintained below  $\sim 10$  nW, so that sub-mK temperatures, perhaps down to about 100  $\mu\text{K}$ , become possible. This requires good rotational symmetry of the apparatus and that it is carefully aligned along the rotation axis.

Table I summarizes some of the solutions chosen in the design of the existing rotating cryostats. They are listed in the order of their commissioning year, which also reflects their technical sophistication. Two aspects have been highlighted in particular: (i) the maintenance of the dilution refrigerator in rotation and (ii) where the analog electronic instrumentation has been placed and how it is connected to the sensors in the cryostat. Both considerations affect in important ways the complexity of the construction work, the ease of operation, and the quality of the rotation and the measuring signals.

The simplest approach to convert a conventional cryostat for rotation is to place the entire installation with pumps and electronics on a large and massive rotating platform. This is adequate for rotation up to 1 rad/s. The Cornell design is closest to this scheme, but here, to avoid vibrations, the mechanical vacuum pumps are located outside the rotating platform. Perhaps the next simplest scheme is that of the Helsinki I cryostat. It avoids rotating vacuum seals by operating the dilution refrigerator in rotation in single-cycle mode with one cryo-adsorption pump. This makes the cryostat autonomous, while it floats on its compressed-air bearings. The only connections from the rotating equipment to the laboratory are (i)

TABLE I

Characteristics of Rotating mK Cryostats. The columns refer to: (i) the appropriate reference; (ii) the year when the cryostat started operating; (iii) the mode in which the dilution refrigerator is operated in rotation [1-Shot Single Cycle or Continuous Recycling]; (iv) how the pumping of the cryostat is organized in rotation [with Rotating Vacuum Seals or by Means of one or Several Alternating Cryo-Adsorption Pumps (cp)]; (v) type of bearings used to support the rotation of the cryostat [1 × Oil—One Horizontal Pressurized Oil Bearing, 3 × Air—One Horizontal Support Bearing and Two Vertical Stabilizing Bearings, Air Pads—Individually Adjusted Air Pads, Usually 3 for Horizontal Support and 3 For Vertical Stabilization, 2 × Air—One Compact Horizontal and One Vertical Air Bearing]; (vi) location of the analog electronics [Rotating with the Cryostat, in a Separate Synchronously Rotating Cradle, or Connected via a Multiple-Slip-Ring Assembly]; (vii) maximum rotation velocity.

Cryostat	Ref.	Start year	Dil. ref.	Pumping	Bearings	Analog instr.	Max $\Omega$ (rad/s)
Berkeley I	11	1973	cont	rot seals	air pads	rotating	1
Cornell	12	1979	cont	rot seals	1 × oil	rotating	0.5
Helsinki I	13	1981	1-shot	1 × cp	3 × air	rotating	4
Helsinki II	14	1988	cont	4 × alt cp	3 × air	synch	6
Berkeley II	15	1990	cont	rot seals	air pads	slip ring	4
Manchester I	16	1990	cont	rot seals	air pads	rotating	2
Manchester II	17	1992	cont	rot seals	air pads	rotating	4
Tokyo I	18	1994	cont	rot seals	2 × air	synch	7
Tokyo II	18	2001	cont	rot seals	2 × air	synch	25

three slip rings for the one-phase mains voltage and ground, (ii) an axial optical data line with one rotating joint on the top of the cryostat and a second on the bottom, (iii) a simple rotating o-ring seal for the He return line from the He dewar to recover the evaporating He gas, and (iv) the rotation drive via a smooth flexible belt. In rotation the only ohmic contact to the electric ground in the laboratory is via the single slip-ring contact.

Most of the cryostats in Table I make use of rotating joints in pumping lines, usually with lightly compressed, but doubly secured O-ring seals, or in later designs with now commercially available magnetic fluid sealed joints. Thus the dilution refrigerator can be operated uninterrupted in the recycling mode, which saves time and work in the daily operating schedule during measurements.

The analog electronics prefers close interference-free connection to the sensors in the cryostat. On the other hand, if this equipment is directly fixed on the rotating cryostat, accurate balancing becomes problematic and mechanical vibrations from cooling fans, for instance, may contribute to vibrational heat leaks. An advanced solution is to place the electronics on a second carousel which is mechanically weakly coupled, but rotates synchronously.

In general such improvements add to the complexity of cryostat construction, increase the vulnerability to failure, demand service, and tend to add to rotational friction. Low friction is advisable for smooth rotation, to reduce vibrations, heat leaks, and interference in measurement. This is especially true if single-vortex resolution should be achieved at a rotation level of a few rad/s, while the rotation noise needs to be  $\langle \Delta\Omega \rangle \lesssim 10^{-3}$  rad/s. It is probably simpler to reduce the influence of friction than to arrange for very stable friction!

### 3. AIR BEARINGS

Smooth rotation is generally supported with oil, gas, or magnetic fluid bearings. Except for the pioneering Cornell design, most cryostats make use of compressed air bearings which provide lower friction. Two alternative approaches to bearing design have been employed: (i) Compact units specially designed to provide horizontal support of the equipment and secondly vertical stability of the rotating axis. At least one of each kind of bearing is used. High-precision machining is required to fabricate these units (which are now also commercially available<sup>18</sup>). In general this approach is thought to provide the best rotation properties at high velocities. (ii) Constructionally simpler is the use of separate thrust pads which are individually adjusted to support a large horizontal plate from which the cryostat is either hanging (Berkeley) or on top of which it has been assembled (Manchester II). Fixed on the plate in its center is a cylindrical vertical surface which with three more horizontally blowing air pads defines and stabilizes the vertical rotation axis.

In both Helsinki cryostats, the rotating equipment is suspended from a central vertical axis which is supported by one large horizontal air bearing. The vertical rigidity of the axis is secured with two vertical bearings above and below the horizontal bearing.<sup>13</sup> In the horizontal bearing compressed air is blown through eight nozzles between two flat  $\varnothing 400$  mm plates. The two vertical bearings are cylindrical  $\varnothing 125$  mm and 70 cm apart from each other. This integrated system of three precision-machined air bearings is one mechanically robust unit which requires little adjustment or maintenance,<sup>13</sup> compared to an assembly of separate individually adjusted air pads. The compressed air at 6 bar pressure has to be filtered to avoid dust particles from collecting in the air bearings. Solid  $\mu\text{m}$ -size particles cause instability in the rotation and have to be removed by flushing alcohol through the bearings. Overall, such a rotation scheme is simple and reliable, shown by the fact that the Helsinki I cryostat is the installation which has been longest in continuous rotating use.

#### 4. ROTATION STABILITY

Although rotation is a most important attribute of the refrigerators in Table I, hardly any published information is available on the quality of their rotation. In this report we describe the rotation noise of the Helsinki I installation. The guide line in its design has been to minimize rotational friction, by avoiding rotating vacuum seals, slip ring assemblies, and other similar components. High-precision stability of the rotational friction is then not required as a function of rotation velocity and time. Large noise attenuation is naturally present, provided by the low-pass filter formed by a loose coupling to the large rotating mass via the flexible belt drive. The belt is under weak tension, but should be tightened sufficiently not to slip excessively in rapid velocity changes.

Ultimately at high rotation, mechanical resonances impair the stability and place an upper safety limit on  $\Omega$ . This depends on the vertical alignment of the apparatus and the rotation symmetry in the distribution of weights. By reducing precession amplitudes and by balancing the weights laterally, noise and stability are improved. In the Helsinki I cryostat these two operations are performed by adjusting differentially the heights of the four cryostat support pillars and by adding lead weights on the rotating cryostat. The quality of the adjustments is judged from the output amplitude of piezo pressure sensors during rotation. These are imbedded in the four vertical cryostat supports and monitor the vertical loading.<sup>13</sup> The ultimate limitation of these adjustments is the uneven weight distribution from the large amount of analog electronic equipment needed for NMR spectrometry. This electronics is fixed on a circular platform which surrounds the upper part of the rotating cryostat. At present with two independent spectrometers, this equipment consists of 18 separate electronics boxes.<sup>19</sup>

The belt drive of the cryostat is pulled by a servo motor which is mounted on the wall outside the electrically shielded cryostat room. It has a maximum shaft output torque of 45 Nm in continuous operation. The servo is operated with a commercial control unit. Its digital feedback loop for speed control obtains the input signal from an optical tachometer monitoring directly the rotating shaft of the motor. The integration time of this PID controller is normally adjusted at  $\sim 8$  ms. Since the cryostat rotation velocities are below 1 Hz and the largest noise components below 10 Hz, an overall feedback loop can still be installed for controlling directly the stability of the cryostat rotation. So far this has not been done.

#### 5. ROTATION NOISE

The measurements with the Helsinki I cryostat on quantized vorticity make use of at least four different modes of rotation: (i) rotation at

constant  $\Omega$  over a length of time (with  $\Omega \lesssim 4$  rad/s), (ii) a slow linear ramp (with  $|\dot{\Omega}| \gtrsim 10^{-4}$  rad/s<sup>2</sup>), (iii) a sudden stop of rotation (with  $|\dot{\Omega}| \sim 1$  rad/s<sup>2</sup>), (iv) sinusoidal modulation  $\Omega(t) = \Omega_0 + \Delta\Omega \sin \omega t$  (with modulation frequency  $\omega \lesssim 2\pi/10$ s and amplitude  $\Delta\Omega \lesssim 1$  rad/s). Modulation of rotation at such high frequencies  $\omega$  and amplitudes  $\Delta\Omega$  requires a drive with large torque while rotation at constant  $\Omega$  demands good stability at small torque.

The rotation  $\Omega(t)$  is recorded with a commercial tachometer unit which has a resolution of 6000 slits/rev. Since the tachometer and its coupling to the cryostat rotation have their own noise limitations, an independent measurement of  $\Omega$  is an important check. Such a reading is obtained from the NMR absorption spectra measured in the vortex-free Landau state of  $^3\text{He-B}$  at different values of  $\Omega$ , as shown in Fig. 1. Here the absorption is seen to shift with increasing  $\Omega$  from the region close to the normal-phase Larmor resonance (approximately at vertical arrow) to a new maximum on the left which arises from the orienting effect of the rotational normal—superfluid counterflow on the order-parameter anisotropy axis. By monitoring the absorption amplitude  $A$  at fixed magnetic field at the

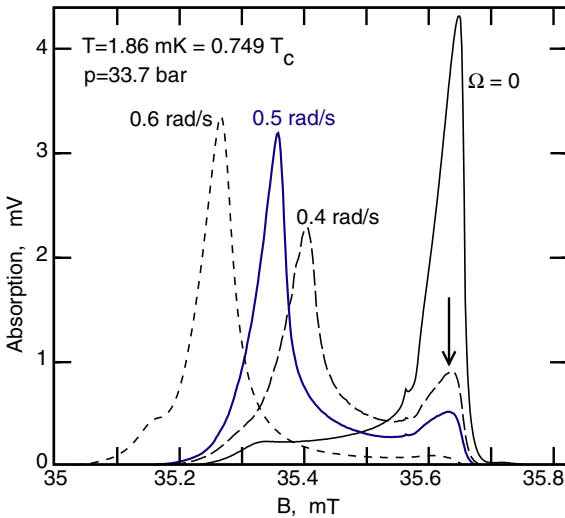


Fig. 1. The NMR absorption spectrum in vortex-free  $^3\text{He-B}$  is a sensitive function of  $\Omega$ . These four spectra at different rotation velocities have been measured at a constant RF excitation frequency of 1.15 MHz, by slowly sweeping the polarizing magnetic field  $B$ . The vertical arrow marks the value of magnetic field at which the absorption amplitude is measured in Fig. 2, to record the rotation noise spectrum.

location of the vertical arrow, the dependence  $A(t) \propto \Omega(t)$  can be used for tachometry.

In Fig. 2 the rotation noise at the tachometer output is compared to that in the simultaneously monitored NMR absorption amplitude  $A(t)$ , measured in the experimental setup of Ref. 19. The two traces are seen to track each other accurately, they reproduce the same noise characteristics,

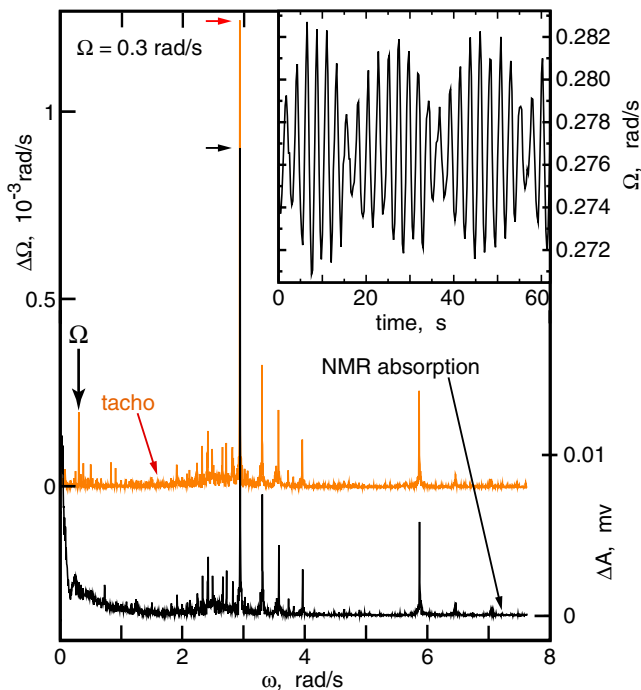


Fig. 2. Rotation noise at constant  $\Omega$ , measured with two different probes. (Top) Fourier spectrum of the tachometer output  $\Omega(t)$ , with the noise amplitude  $\Delta\Omega$  plotted as a function of the fluctuation frequency  $\omega$ . The peak at the lowest frequency  $\omega \approx 0.3$  rad/s arises from some residual coupling to the rotation velocity  $\Omega$ . (Bottom) Corresponding spectrum of the NMR absorption amplitude  $A(t)$ , given as  $\Delta A$  versus  $\omega$ . The two plots show that the measurements give identical results. Both spectra have been recorded by accumulating data for 1500 s, with 4 readings per second, at  $\Omega = 0.3$  rad/s. The prominent peak at  $\omega \approx 2.9$  rad/s (or 0.47 Hz) with an amplitude  $\Delta\Omega \approx 1.3 \cdot 10^{-3}$  rad/s (horizontal arrows) is the largest mechanical resonance in the rotation of the cryostat. (Insert) Tachometer reading as a function of time  $t$  at  $\bar{\Omega} = 0.277$  rad/s. The overall appearance of the noise is a sine wave at the frequency  $\omega \approx 2.9$  rad/s, which is modulated by the frequency of the rotation  $\omega = \Omega$ . The amplitude and frequency of the dominant mechanical resonance depend on the balancing and alignment of the cryostat. (In the insert  $\omega \approx 2.7$  rad/s.)

and thus the tachometer reading represents a reliable measurement of rotation noise. This statement is not trivial since the noise peaks are on the level  $\Delta\Omega/\Omega \gtrsim 10^{-4}$  and could be distorted by tachometer problems.

The noise spectra in Figs. 2 and 3 show that at about 0.3 rad/s the noise is characterized by a series of sharp resonances, with Q values of order 100. The largest one, at  $\omega \approx 3.0$  rad/s, has also a sizeable second harmonic. Isolated mechanical resonances of this kind are typical of rotating machinery at low  $\Omega$  where the angular momentum does not yet smooth out instabilities. At somewhat higher  $\Omega$  the resonances are not as dominant and the quality of rotation is at its best. At still higher  $\Omega$  the broad-band noise starts to grow. Here also new resonances appear with growing amplitudes and increasingly closer spacing, when the mechanical stability of the apparatus starts to suffer from insufficient rotational balancing. This change over in the character of the noise is illustrated in Fig. 4, where  $\Omega$  is slowly increased at constant rate  $\dot{\Omega}$ . At present we suspect that part of the noise arises from a coupling to the vibrational modes of the four steel support pillars of the rotating equipment. For a detailed analysis one needs to correlate simultaneous measurements of rotation with the tachometer and of vibrations with an accelerometer.

These noise characteristics are typical of the Helsinki I cryostat. The locations and magnitudes of the noise resonances can be moved around by

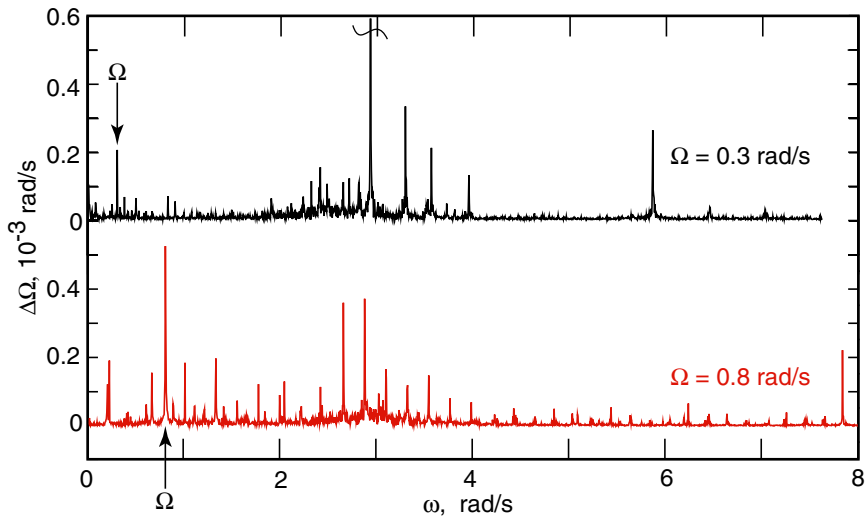


Fig. 3. Rotation noise at two constant values of  $\Omega$ , recorded with the tachometer. (Top) For reference, the same Fourier spectrum as in Fig. 2 (top), with the largest peak truncated. (Bottom) At somewhat higher  $\Omega$  in the “quiet regime” all resonances are smaller in amplitude than the peak at the frequency of rotation  $\omega = \Omega = 0.8$  rad/s.

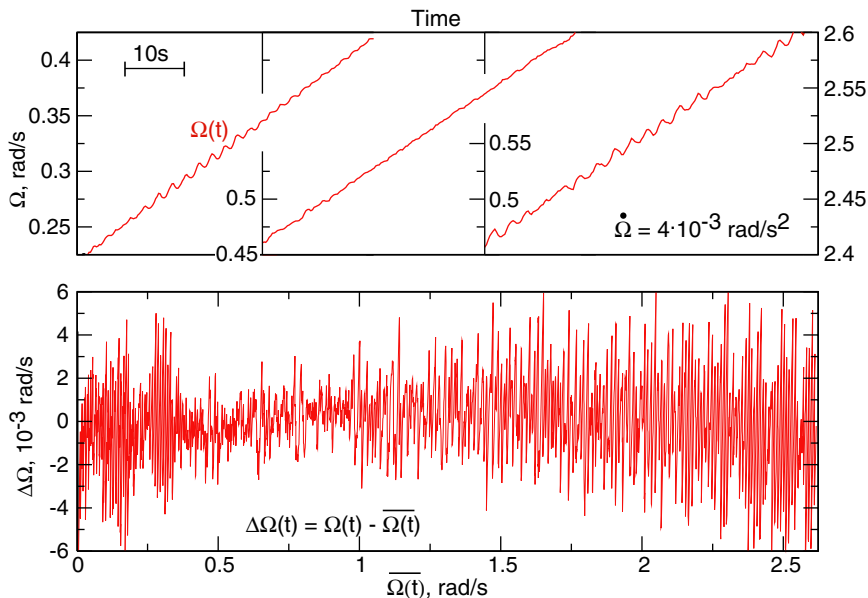


Fig. 4. Noise in slowly increasing rotation. (Top) Three separated sections of one continuous linear ramp at  $\dot{\Omega} = 4 \cdot 10^{-3} \text{ rad/s}^2$  illustrate the changing nature of noise in these three rotation regimes. (Bottom) Deviations of the measured  $\Omega(t)$  from a linear fit  $\overline{\Omega(t)}$  over the entire  $\Omega$  range, as a function of rotation  $\Omega$ : (i) at low  $\Omega < 0.4 \text{ rad/s}$  dominates the mechanical resonance of the cryostat at  $\omega \approx 2.9 \text{ rad/s}$ , (ii) at intermediate velocities  $0.4 \text{ rad/s} < \Omega < 1.4 \text{ rad/s}$  is the “quiet regime,” and (iii) at high velocities  $\Omega > 1.4 \text{ rad/s}$  the stability limit of the rotating installation is approached.

removing and adding weight on the rotating equipment and by adjusting the tightness of the drive belt. It is instructive to look at the properties of one of these resonances. At low rotation  $\Omega < 0.4 \text{ rad/s}$  the noise is dominated by one sharp resonance with the frequency  $\omega \approx 3 \text{ rad/s}$  or  $0.5 \text{ Hz}$  (Fig. 2). Its peak height varies as a function of  $\Omega$  such that weak maxima appear at least at  $0.145$  and  $0.29 \text{ rad/s}$  (Fig. 5 (top)). The tachometer output shows a well-resolved oscillation at this frequency (Fig. 2 (insert)). This oscillation is modulated by a second frequency which is the rotation velocity itself. The peak-to-valley modulation depth is of order 3:1. If the tension in the drive belt is reduced, the frequency of the dominant noise peak decreases by only small amounts, but its amplitude can be made to essentially disappear (Fig. 5 (bottom)). We interpret this to mean that the resonance characterizes a mechanical mode in the rotating equipment assembly. This mode functions as a tuned amplifier which picks its

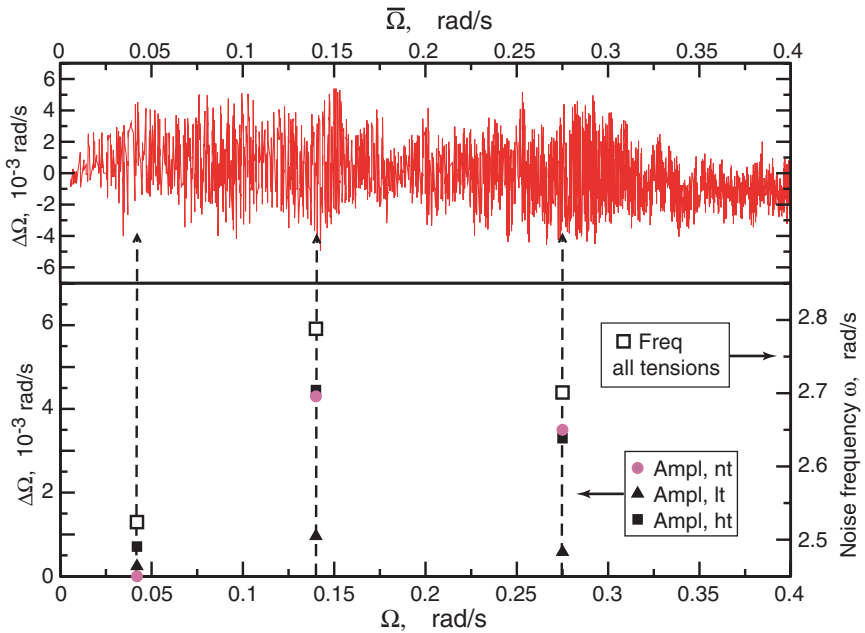


Fig. 5. Analysis of the largest noise resonance at low rotation velocity. (Top) Similar to Fig. 4, the deviations of the measured  $\Omega(t)$  from a linear fit  $\bar{\Omega}(t)$  are plotted as a function of  $\bar{\Omega}(t)$  at low  $\Omega \leq 0.4$  rad/s. The largest noise component in this regime is the dominant mechanical resonance of the cryostat, here at  $\omega \approx 2.7$  rad/s or 0.43 Hz. The small change from  $\omega \approx 2.9$  rad/s in Fig. 2 is caused by differences in the cryostat balancing and alignment. (Bottom) Influence of the tension in the drive belt on the dominant noise resonance. The amplitude and frequency of the dominant resonance, determined from the Fourier spectrum, have been plotted at three different levels of tension: (i) at the normally used intermediate tension (nt), adjusted to track rapid changes in rotation velocity, (ii) at the lowest possible tension (lt), and (iii) at high maximum tension (ht). The amplitude of the noise resonance depends strongly on tension while the frequency changes relatively much less. Overall the noise amplitude thus depends on (i) the rotation velocity  $\Omega$ , on (ii) the tension of the belt, and on (iii) adjustments performed on the cryostat for alignment and balancing. The resonance we believe to be a high Q mode of the rotating refrigerator.

excitation from the broad-band noise transmitted over the drive belt. The modulation of the noise peak reflects the influence of the angular position of the cryostat on the mechanical resonator, via a precessing component in the motion or a departure from rotational symmetry in the balancing of the weights.

## 6. SINGLE-VORTEX RESOLUTION IN ROTATION

In bulk samples single-vortex resolution is possible to achieve since the superfluid circulation quantum  $\kappa_0 = h/M$  is a macroscopic quantity, in

spite of the fact that it is the ratio of two numbers of atomic scale, Planck's constant  $h$  and the mass  $M$  of the superfluid particle (for  $^3\text{He}$ :  $M = 2m_3$  and  $\kappa_0 = 0.0662 \text{ mm}^2/\text{s}$ ). Such measurements have been an important tool in the study of quantized vorticity in the  $^3\text{He}$  superfluids, where one needs to distinguish between different vortex structures. The usual case is one where the critical velocity of vortex formation  $v_c = \Omega_c R$  is constant as a function of  $\Omega$ . Here we denote the rotation velocity at which the first vortex is formed with  $\Omega_c$ , i.e., when the number of vortex lines is still  $N = 0$ . In contrast, the equilibrium state in rotation carries an areal density  $n_v = 2\Omega/\kappa$  of rectilinear vortex lines, where  $\kappa = \nu\kappa_0$  and  $\nu$  is the quantization number of a vortex line. Using the simplest approximation, we write the total number of rectilinear vortex lines in the equilibrium state as  $N_{\text{eq}} = \pi R^2 n_v$ .

A state  $N(\Omega)$  with less than the equilibrium number of vortex lines consists of a central vortex cluster where the  $N$  vortex lines are compressed to the equilibrium areal density  $2\Omega/\kappa$  by the rotational counterflow which circulates around the cluster with the velocity  $v = v_n - v_s = \Omega r - \kappa N / (2\pi r)$ , where  $R_v \leq r \leq R$  and  $R_v = \sqrt{\kappa N / (2\pi\Omega)}$  is the radius of the vortex cluster. Here the second term, the superfluid velocity outside the cluster, is simply equivalent to the flow around a single giant vortex with the circulation  $\kappa N$ . Assuming that the vortices are formed at the outer boundary of the sample, the critical velocity  $v_c$  is as a function of  $\Omega$

$$v_c = \Omega_c R = \Omega R - \frac{\kappa N}{2\pi R}.$$

In a measurement of the total number of vortex lines  $N(\Omega)$ , we get from this equation the slope  $dN/d\Omega = 2\pi R^2/\kappa$ , assuming that  $v_c$  is constant. Equivalently, the rotation increment per each new vortex line is  $\Delta\Omega = \nu\kappa_0 / (2\pi R^2)$ . By measuring this increment, the quantization number  $\nu$  is obtained. Moreover, if  $v_c$  is a constant and we have determined the number of vortex lines  $N_1$  at some rotation velocity  $\Omega_1$ , then we find from the above relation the critical value  $\Omega_c$  (and vice versa).

In NMR absorption measurements it is often possible to identify an absorption peak whose amplitude and intensity are directly proportional to the change in  $N$ , at least within some limits.<sup>20</sup> For intrinsic processes the critical velocity  $v_c$  is a constant for the singly quantized vortex lines ( $\nu = 1$ ) in  $^3\text{He-B}$ .<sup>5</sup> In  $^3\text{He-A}$  this is not necessarily the case: Here the isolated vortex line, which is formed in slowly increasing rotation, is doubly quantized<sup>21</sup> ( $\nu = 2$ ). Its critical velocity depends on the global order parameter texture.<sup>6</sup> If the texture is stable, then  $v_c$  is constant. However, occasionally one may encounter a discontinuous jump to a different, usually smaller value of  $v_c$ .

Here the texture undergoes a transition to a different, usually less perfect configuration. For the equilibrium vortex sheet the critical velocity is inherently nonlinear:  $v_c \propto \sqrt{\Omega}$ .

As seen from the rotation increment required per vortex line,  $\Delta\Omega = \kappa/(2\pi R^2)$ , by reducing the sample radius  $R$  the stability and noise requirements on  $\Omega$  become less stringent, but simultaneously the required rotation velocities increase:  $\Omega_c = v_c/R$ . Unlike in  $^3\text{He-B}$ , in bulk-liquid-like samples of  $^3\text{He-A}$  critical velocities are low and this option for increasing the resolution was used in Ref. 21. Recent measurements with the Tokyo I cryostat illustrate these dependences further.<sup>8</sup> It was found that for a sample of  $^3\text{He-A}$  with a diameter of 0.2 mm the critical velocity for forming the first vortex line was  $\Omega_c \sim 4.8$  rad/s. The velocity for forming the second vortex line, presumably  $\sim 9.6$  rad/s, was already beyond the upper safe limit of rotation. This measured value of  $v_c$  is, nevertheless, 20% lower than  $\Omega_c \approx 0.32$  rad/s, which was measured consistently in Ref. 22 for a sample of 3.9 mm diameter (see Fig. 6), and it is only about one third of the maximum critical velocities recorded in the more extensive studies of Ref. 6. Since  $v_c$  in  $^3\text{He-A}$  is determined by the global order parameter texture, variations of this magnitude are usual.<sup>6</sup> Thus the dominant vortex in a 0.2 mm sample appears to match the characteristics of the same doubly quantized vortex which is observed in samples of larger diameter.

In  $^3\text{He-B}$  the critical velocity is much higher, but depends on surface roughness. In the presence of smooth surfaces  $v_c$  might be pushed up into the noisy rotation regime of the cryostat or even above the upper safe limit. However, on warming towards  $T_c$ ,  $v_c$  rapidly decreases, owing to the temperature dependence  $v_{cB} \propto \sqrt{1-T/T_c}$  in the Ginzburg-Landau temperature range. Thus a suitable velocity regime might be found by adjusting the temperature.<sup>5</sup> It should be noted that all these velocities in the  $^3\text{He}$  superfluids are orders of magnitude higher than the Feynman critical velocity  $\Omega_{c1} = \kappa/(2\pi R^2) \ln(R/\xi)$ , where  $\xi$  is the vortex core radius. This is the rotation velocity at which the first rectilinear vortex line becomes energetically more favorable than the vortex-free state.

## 7. REQUIREMENTS ON ROTATION NOISE

To resolve the addition of one new vortex to a bulk sample with a large number of already existing rectilinear vortex lines, a limit on the allowed rotation noise amplitude can be given. The reduction in counterflow velocity at the cylindrical sample boundary per each new vortex line is  $\Delta\Omega = \kappa/(2\pi R^2) \approx 3 \cdot 10^{-3}$  rad/s for a  $^3\text{He-B}$  sample with a 2 mm radius  $R$ . The addition of one new vortex line can thus be seen as a small discontinuous change in the absorption amplitude measurement of Fig. 1.

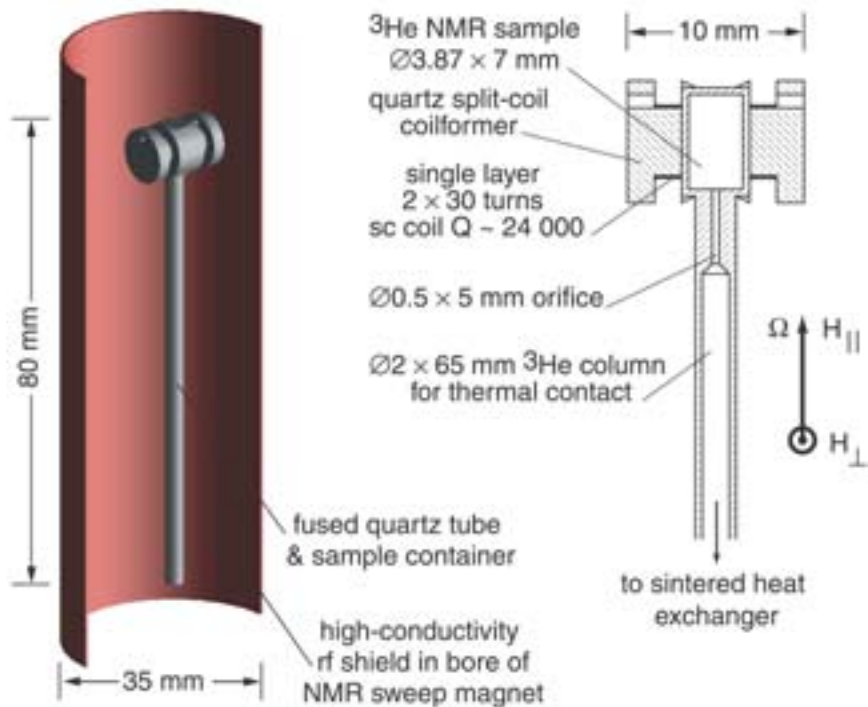


Fig. 6. NMR measuring setup for  $^3\text{He}$  sample in the rotating cryostat.<sup>22</sup> This arrangement demonstrates a subtle interference signal from rotation: The superconducting NMR pick-up coil is located at the top end of a long quartz tube which is fixed at its lower end to the nuclear cooling stage (located below this NMR setup). The surrounding high-conductivity copper RF shield coats the bore of the brass coil former of the superconducting NMR polarizing magnet which in turn is fixed at its top end to the mixing chamber (located above this NMR setup). In precessing rotation, gravity causes a differential oscillation of  $\mu\text{m}$ -size amplitude between the pick-up coil and the shield. This linear oscillation modulates the properties of the NMR tank circuit. The modulation is phase locked to the rotation, as can be seen in the absorption response in Fig. 7. The modulation amplitude changes with the differential height adjustment of the four pillars, which support the cryostat, and depends thus on how vertically the NMR set up has been adjusted.

This requires sufficient sensitivity in the NMR absorption measurement, to resolve a small discontinuous change in absorption, but equally importantly the  $\Omega$  noise has to be in amplitude well below the above value of  $\Delta\Omega$ . In this way the critical velocity was measured for  $^3\text{He-B}$  as a single-vortex phenomenon in Ref. 5. The equivalent measurement in  $^3\text{He-A}$  is more difficult because of a smaller absorption amplitude increment per each new vortex line. In the quiet  $\Omega$  regime of the cryostat the measurement could be

performed with the measuring setup shown in Fig. 6, which was used in the measurements of Refs. 21 and 22.

The critical velocity of vortex formation is measured in slowly increasing rotation, while the annihilation threshold is recorded in slowly decreasing rotation.<sup>21</sup> The total vortex number, in turn, is usually determined by comparing absorption spectra at constant rotation at some value  $\Omega_{\text{ref}}$ . Here one has to return many times to the same reference velocity  $\Omega_{\text{ref}}$ , after intervening manipulations at other  $\Omega$  values. Thus the precision in readjusting  $\Omega_{\text{ref}}$  and the stability of rotation at  $\Omega_{\text{ref}}$  determine the accuracy with which the number of vortex lines can be obtained.<sup>23</sup>

Rotation noise does not only blur the  $\Omega$  value to which the formation or annihilation of a vortex line should be ascribed. It also couples to the absorption measurement: (i) It may contribute directly to the noise amplitude of the measuring signal via changes in  $\Omega$  and their influence on the order-parameter texture. A straightforward example is the case of Fig. 2, but more subtle changes occur in the NMR spectra of  $^3\text{He-A}$ .<sup>22</sup> (ii) Vibrations associated with large resonances may couple mechanically into the measurement and modulate directly the measuring signals via differential mechanical motion of the sample, the measuring probes, or the environment. (iii) Recently it was established that in  $^3\text{He-B}$  at temperatures  $< 0.6 T_c$ , where mutual-friction damping of vortices has dropped below a critical level, the geometrical depinning of vortex lines from the edge of the container orifice is directly affected by the large mechanical resonance at the noise frequency  $\omega \approx 2.9$  rad/s in Fig. 2. The depinning is observed as a sudden leakage of vortices from the heat exchanger volume, which is filled with the equilibrium areal density of vortex lines, through the orifice into the vortex-free sample volume at about  $\Omega \sim 0.3$  rad/s.<sup>24</sup> The orifice (also present in Fig. 6) is needed to fill the sample volume and to provide the thermal connection between the sample and the heat exchanger.

An example of the interference problems, which arise from rotation, is the following: Precessing rotation, as a first approximation, is a superposition of rotation and linear oscillation. Figures 6 and 7 describe an instructive demonstration how the linear pendulum motion may interfere in rotating measurements. The NMR absorption signal in Fig. 7 is distorted by a sinusoidal modulation which is phase locked to the rotation. For a long time we searched for a direct electrical cause for this interference. These efforts proved frustratingly fruitless, until it was found that by adjusting the vertical alignment of the rotation axis the amplitude of the modulation changed and could be made to vanish (except perhaps a residue from a 2nd harmonic). This indicates that it is the linear oscillation in the gravitational field which is here recorded via a differential motion of the high-Q NMR detection coil with respect to its conducting environment.

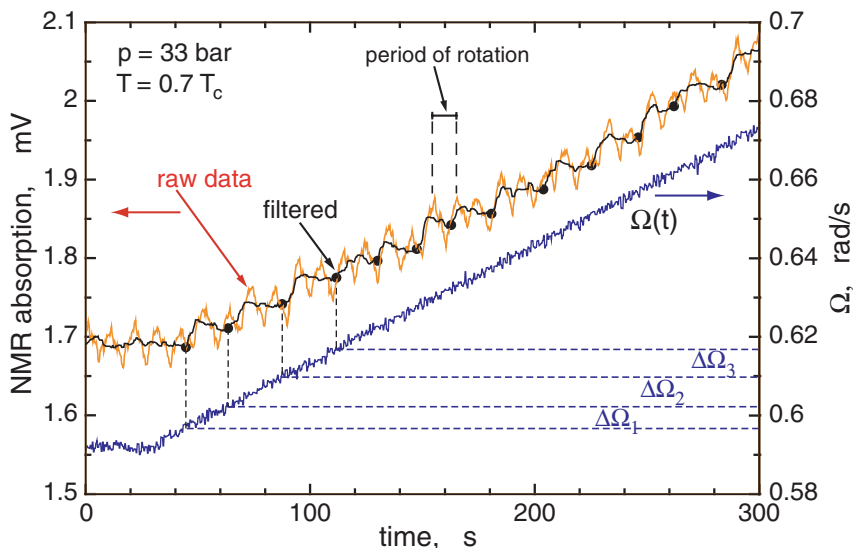


Fig. 7. Measurement of vortex formation in  $^3\text{He-A}$ .<sup>21</sup> The plot illustrates modulation of the NMR absorption by precessing rotation. The bottom trace is the rotation drive  $\Omega(t)$  as a function of time  $t$ . In this plot the velocity of the normal—superfluid counterflow,  $|v_s - v_n|_{r=R}$  at the cylindrical sample boundary, is close to the constant critical value at which a vortex line is formed. When the drive  $\Omega(t)$  starts to increase on the left at  $t \approx 40$  s, the absorption amplitude (marked as “raw data”) also starts increasing correspondingly on an average. It is disguised by a superimposed periodic signal which is accurately phase locked to the rotation. Using a digital notch filter centered at the frequency  $\Omega(t)$  and its harmonics, a staircase pattern is revealed in the “filtered” absorption signal. It arises when one rectilinear vortex line after another is periodically formed as a function of  $\Omega$  at a constant critical counterflow velocity  $|v_s - v_n|_{c,r=R}$ . The black dots have been plotted to emphasize the increment  $\Delta\Omega$  per each newly formed vortex line. The average value of  $\Delta\Omega \propto \nu\kappa_0$  allows a direct determination of the quantization  $\nu$  of circulation per vortex. Here it was found that  $\nu = 2$  and thus the dominant vortex line in  $^3\text{He-A}$  is doubly quantized.

**Final Note.** A large number of different technical solutions are available today from which to choose in the design of a rotating cryostat. Few studies exist about their relative merits. Depending on the planned experiments, design choices may differ. We have pointed out in this report one important consideration, the need to secure sufficiently noise-free rotation properties so that precision measurements of quantized vorticity become possible. This aspect will become more demanding in future measurements at ever higher rotation velocities. It would be useful to complement the present studies of rotation noise with similar information about other rotating refrigerators and about simple techniques how to suppress

their dominant noise resonances. Such information would be helpful when new cryostat constructions are planned or existing apparatus is rebuilt to meet new demands.

### ACKNOWLEDGMENTS

We thank the research community listed in Table I for valuable discussions and instructive comments concerning this report. This collaboration was carried out under the EU-IHP ULTI 3 visitor program and the ESF COSLAB and VORTEX conference programs.

### REFERENCES

1. E. L. Andronikashvili and Y. G. Mamaladze, in *Progress in Low Temperature Physics* Vol. V, North-Holland, Amsterdam (1967), p. 79.
2. D. V. Osborne, *Proc. Phys. Soc. A* **63**, 909 (1950).
3. H. E. Hall, *Adv. Phys.* **9**, 89 (1960).
4. V. B. Eltsov and M. Krusius, in *Topological Defects in  $^3\text{He}$  Superfluids and the Non-Equilibrium Dynamics of Symmetry-Breaking Phase Transitions*, Y. Bunkov and H. Godfrin (eds.), Kluwer, Dordrecht (2000), p. 325.
5. Ü. Parts *et al.*, *Europhys. Lett.* **31**, 449 (1995); V. M. H. Ruutu *et al.*, *J. Low Temp. Phys.* **107**, 93 (1997).
6. V. M. H. Ruutu *et al.*, *Phys. Rev. Lett.* **79**, 5058 (1997).
7. J. S. Korhonen *et al.*, *Phys. Rev. Lett.* **65**, 1211 (1990).
8. R. Ishiguro, O. Ishikawa, M. Yamashita, and Y. Sasaki *et al.*, submitted to *Phys. Rev. Lett.*; *Physica B* **329–333**, Part 1 (2003).
9. T. Kita, *Phys. Rev. Lett.* **86**, 834 (2001).
10. W. F. Vinen and J. J. Niemela, *J. Low Temp. Phys.* **128**, 167 (2002).
11. G. A. Williams, R. E. Packard, *J. Low Temp. Phys.* **39**, 553 (1980).
12. B. C. Crooker *et al.*, *Physica B* **108**, 795 (1981).
13. P. J. Hakonen *et al.*, *Cryogenics* **23**, 243 (1983).
14. R. H. Salmelin *et al.*, *J. Low Temp. Phys.* **76**, 83 (1989).
15. J. D. Close *et al.*, *Physica B* **165–166**, 57 (1990).
16. M. R. Ardron *et al.*, *Physica B* **165–166**, 55 (1990).
17. H. E. Hall *et al.*, *Physica B* **194–196**, 41 (1994).
18. M. Kubota, T. Obata, and R. Ishiguro *et al.*, *Physica B* **329–333**, Part 1 (2003).
19. R. Blaauwgeers *et al.*, *Phys. Rev. Lett.* **89**, 155301 (2002); *Physica B* **329–333**, Part 1 (2003).
20. V. M. H. Ruutu *et al.*, *J. Low Temp. Phys.* **103**, 331 (1996).
21. R. Blaauwgeers *et al.*, *Nature* **404**, 471 (2000).
22. V. B. Eltsov *et al.*, *J. Low Temp. Phys.* **124**, 123 (2001).
23. V. M. Ruutu *et al.*, *Phys. Rev. B* **56**, 14089 (1997); *Physica B* **255**, 27 (1998).
24. L. Skrbek *et al.*, *Physica B* **329–333**, Part 1, p. 106 (2003).